PROCEEDINGS OF SCIENCE

Muography

Hiroyuki K.M. Tanaka[1]
Earthquake Research Institute, The University of Tokyo
1-1-1 Yayoi, Bunkyo, Tokyo 113-0032
E-mail: `ht@riken.jp`

High-energy muons in cosmic rays can be used as a radiographic probe to explore the internal structure of gigantic objects. This new subterranean imaging technique called muography can serve as a new and alternative high-resolution imaging technique, providing a fresh approach to Earth studies. This brief review focuses on recent developments of muography and their results are summarized here, and anticipated future observation prospects are also discussed.

The 3rd International Symposium on "Quest for the Origin of Particles and the Universe"
5-7 January 2017
Nagoya University, Japan

[1]Speaker

PoS(KMI2017)026

1. Introduction

Muography is a technique that uses high-energy muons as a radiographic probe to image the internal structure of gigantic objects. Since high-energy muons have a stronger penetration power than X-rays, this technique can create projection images of hectometric to kilometric sized objects. Although there are limitations to the targetable size of the objects that can be imaged by muography, researchers have applied this technique to various scientific targets that include volcanoes [such as Asama, Japan [1-3], Satsuma-Iwojima, Japan [4, 5], Showa-shinzan, Japan [6], Usu, Japan [7], Unzen, Japan [8], La Sourfiere, France [9, 10], Puy de Dome, France [11], Stromboli, Italy [12] and Etna, Italy [13, 14]], seismic faults in Japan [15, 16], ancient architecture [such as the Egyptian pyramids [17-19], and Mt. Echia, Italy [20]], and industrial plants [including electric furnaces [21] and nuclear reactors [22]].

The idea of using muons produced from cosmic rays was first applied by E.P. George [23]. He measured the thickness of the rock overburden of a tunnel in Australia with a Geiger counter. George was unable to obtain imagery data from his experiment, however his idea was adapted by Luis Alvarez [17] with the intention of recording a muographic image. He installed his spark chamber in the Belzoni Chamber inside Chephren's pyramid and tried to image a hidden chamber that was suspected to be inside the pyramid. Although new chambers were not discovered in this pyramid, his pioneering work triggered a recent modern muographic challenge: the ScanPyramid project inside Kufu's pyramid [18].

The first experimental mugoraphic evidence focused on the top part of Mount Asama, Japan in 2006. Collaboration between The University of Tokyo and Nagoya University recorded muon tracks by using the technique of nuclear emulsions, which was developed for the OPERA (Oscillation Project with Emulsion-tRacking Apparatus) project [24]. The resultant muographic image showed for the first time the strengths of this technique: its suitability to image structures with non-uniform density, and its wide range of applicability in situations when it is essential to characterize a density profile. In this article, the focus will be on the principle and recent developments in the field of muography and its future potential will be discussed.

2. Principle

Muons are generated in the interaction between primary cosmic rays and atmospheric nuclei such as nitrogen or oxygen. The primary directional information of cosmic rays is lost after many twists and turns inside the Galactic magnetic field. These primary particles are isotropically incident from the top of the atmosphere. The resultant products, such as pions and kaons, eventually decay into muons and neutrinos (Figure 1). The differential atmospheric muon spectrum at various zenith angles has been measured with the DEIS [25], BESS [26], KIEL-DESY [27], L3+C [28], and MUTRON [29] experiments. A higher flux is observed for the vertical muons but the average muon energy decreases. There are fewer but, higher energy muons are observed at larger angles (from the zenith) because horizontal pions and kaons decay more before further interactions.

PoS(KMI2017)026

Charged pions $\pi^{\pm} \rightarrow \mu^{\pm} + \nu_{\mu}(\overline{\nu}_{\mu})$ (~100%)

Neutral pions $K^{\pm} \rightarrow \mu^{\pm} + \nu_{\mu}(\overline{\nu}_{\mu})$ (~63.6%)

Neutral Kaons $K_{L} \rightarrow \pi^{\pm} + e^{\pm} + \nu_{e}(\overline{\nu}_{e})$ (~40.6%)

Neutral Kaons $K_{L} \rightarrow \pi^{\pm} + \mu^{\pm} + \nu_{\mu}(\overline{\nu}_{\mu})$ (~27.0%)

Neutral Kaons $K_{S} \rightarrow \pi^{+} + \pi^{-}$ (~69.2%)

Figure 1: Decay modes of pions and kaons to muons. The numbers indicate the branching ratios. The neutral kaons also contribute to the production of muons via the pion decay.

Muons in matter lose their energy via ionization, bremsstrahlung, direct pair production, and photonuclear interactions. The ionization process is called the continuous process because muons frequently collide with electrons, losing a very small fraction of their energy in each collision. The other three processes are called the stochastic process because muons lose a large but random fraction of their energy, and thus fluctuations within this range are enhanced by these processes. For muons with energies below a few hundred GeV, the contribution of the ionization process is dominant when compared with other three processes, so it is convenient to use the continuous slowing down approximation (CSDA) range [30] for estimating the muon flux after passing through the target object.

The minimum energy (E_c) of the muons that can pass through the target object can be calculated when both the muon path length and the average density along the path are known, and the results can be incorporated in the open-sky muon spectrum. By integrating the open-sky spectrum from E_c to infinity, we obtain the integrated muon flux, which represents the number of muons that have enough energy to escape from the target (Figure. 2).

Therefore, by measuring the numbers and arrival directions of muons, the angular distribution of E_c will be obtained, and for this, various kinds of detectors including scintillators [31], micro-mesh gaseous structure (MICROMEGAS) [19], glass resistive plate chambers (GRPC) [11], multiwire proportional counter (MWPC) [32], and nuclear emulsions [1] have been used for tracking muons to generate muographic images.

Although the muon's angular distribution becomes broader as it propagates through matter, its spread is suppressed to ~12 mrad half width at half maximum (HWHM) [33]. The highly penetrating nature of high-energy muons, coupled with their low divergence enable us to generate the density distribution along the muon paths.

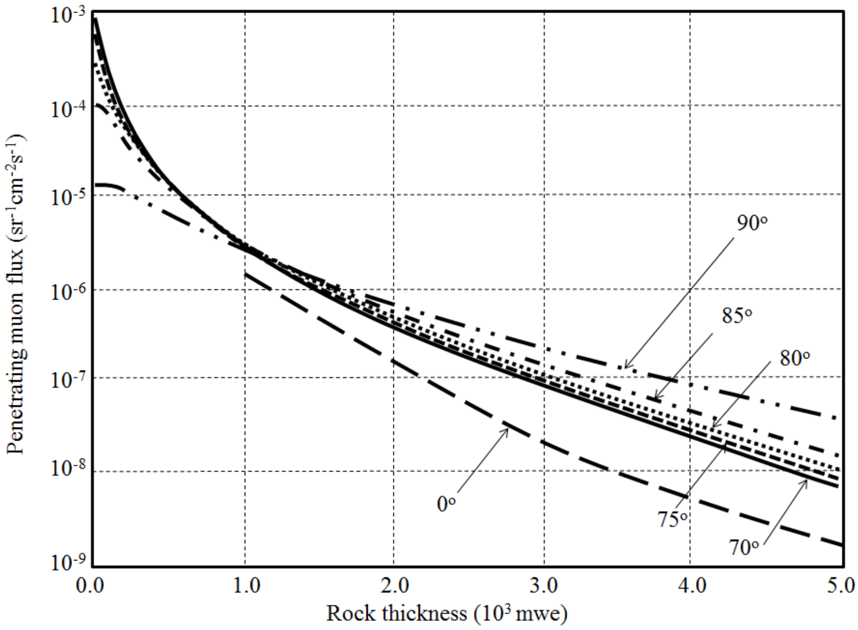

Figure 2: Integrated muon flux after passing through the rock with a given thickness in units of meter water equivalent (mwe). The angles are measured from the zenith.

3.Recent developments

3.1 Dynamic muography

While static muographic images provide useful structural information, the capability to obtain dynamic, sequential images of the temporal variations inside the target objects provide more insight into the processes. This is possible because muons are precipitating almost constantly and continuously [10]. The first trial of this approach was attempted in Asama in 2009 [2]. During the muographic observation, Asama erupted on 2 Feb 2009, and a reduction in the size of the old magma deposit was detected by comparing the images before and after the eruption. (Figure 3). In conjunction with a petrological study of the 2009 eruption ejecta that indicated the same chemical composition of the magma deposit created in the 2004 eruption, it was interpreted that high-pressure vapor blasted through the old magma deposit, which had acted as a “plug” in the pathway.

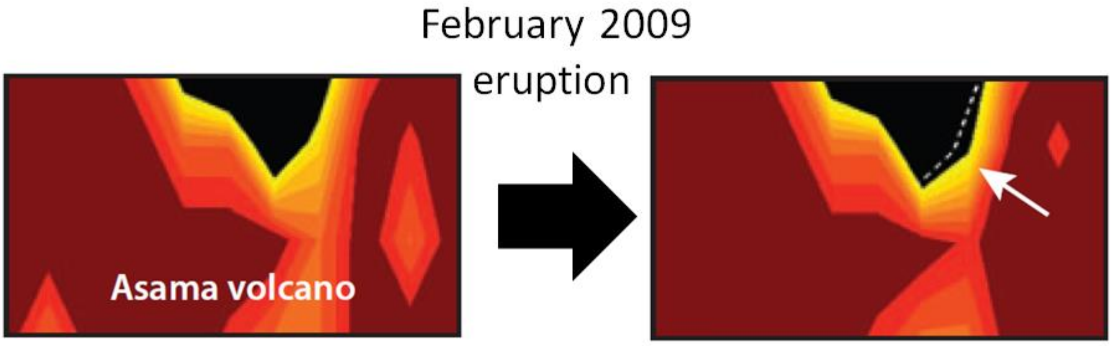

Figure 3: Muographic image of Asama volcano, Japan. The images were taken before and after 2009 eruption. The dashed line indicates the shape of the crater before the eruption. The images indicate the disappearance of the northern section of the magma deposit.

More recent achievements of dynamic muography include the visualization of the ascent and descent of magma column during the 2013 Satsuma-Iowjima eruption [5]. These time-sequential muographic images captured the process as the top of a magma column approached the crater floor during the period from 14–16 June, 2013. On 16 June, a white-colored eruption column was ejected from the vent, rising to a height of 400 m above the crater rim, and during night-time of the same day, a volcanic glow was observed. Volcanic glows are observed during the night when a crater floor is heated, and indicates that magma has approached the ground surface. From 29 June to 1 July, similar muographic images were taken. Once again, on 30 July, a white-colored eruption column was ejected and reached 200 m above the crater rim. Volcanic glow was again recorded. A similar trial to measure the time-dependent variations in muon flux, was attempted in La Soufrière of Guadeloupe, France and a potential application of muography for monitoring temporal changes caused by the hydrothermal movements inside the lava dome was explored [10]. Signals that indicated the volcanic activities were detected beyond the expected muon modulation due to atmospheric effects, and it was interpreted to have been caused by fluid transportation in the hydrothermal system.

3.2 Tomography

Multi-directional muography enables us to reconstruct 3-dimensional slices of the target volume (tomography). However, appropriate locations to place muon detectors are not easily found in volcanic areas for various reasons (e.g., accessibility, infrastructures, etc.), and thus far, bi-directional muography has been the best possible solution to infer the 3-dimensional structure of Asama [3], La Soufriere [10], and Puy de Dome [11], In La Soufriere, the bi-directional muographic images were compared with the soil resistivity data and in Asama, the 3-dimensional structures were reconstructed by processing 2 different images. The 3 dimensional information is useful to diagnose the volcanic activities because (A) the volcano is in general heterogeneous and not axi-symmetric, and (B) it makes simpler to compare with other geophysical data (e.g. seismic tomography or soil resitivity) that usually provide the three dimensionl slice of the target objects.

For example, in Asama, it was found that the pathway of magma was shifted towards the north direction, which explains why recent Asama eruptions tended to eject material in the north direction (Figure 4). This is also consistent with the 2009 muographic result that indicated an explosion of a north part of the crater floor [2]. However, reconstruction with a small number of images requires various assumptions such as the exterior shapes of the target volume, the location of the density of the anomaly, and the size and shape of the anomalies for reconstruction.

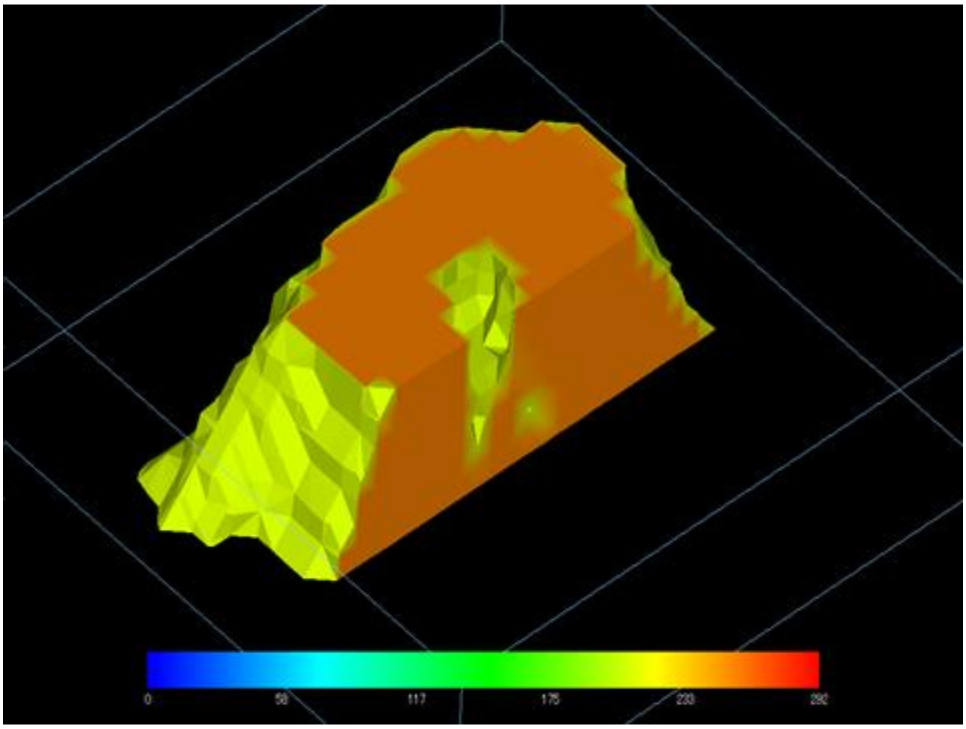

Figure 4: Three-dimensional slice of Asama. Lower right of the image is the north direction.

An availability of the space for muon detectors in volcanic areas is mostly limited to the geographical and infrastructural conditions. Airborne muography may remove these restrictions. In particular, heliborne muography makes it possible for us to transport the detector to the observation point along with electric supply. Heliborne muography detectors are operated inside a helicopter that hovers at the observation point and the data are collected at the same time (Figure 5). The time required for the data collection is shortened by approaching the target object as close as possible. In the first experiment of its kind, the muographic image was taken in 2.5 hours near the Heisei-Shinzan lava dome, Kyusyu, Japan, and the high density spine was distinguishable from the surrounding flactured sediments [8]. Future multi-direction heliborne muography will improve the quality of tomographic images.

Figure 5: Heliborne muography in Heisei-Shinzan lava dome, Japan. A complete (upper panel) and closer (lower panel) views are shown. The helicopter hovered and its position was measured with the global positioning system (GPS). Heliborne muography makes it possible to conduct an observation near a sheer precipice.

4.Conclusion

The technique of volcano muography is directly applicable to other target objects. The internal structures of the Egyptian pyramids are recently attracting researcher's interests. It intrigued Luis Alvarez 50 years ago, and now intrigues physicists and multi-media scientists. Improvements to the muography technique that was not available 50 years ago now start to reveal the undiscovered structures in the Cheops pyramid. However, currently only a projection image is available, and thus it is difficult to judge if the discovered region represents a completely open space or just a region in which low density materials were used. More precise three dimensional structures will be required in the future. For this, high definition 3-dimensional muographic images may be useful, which will be available by utilizing high position sensitive muon detectors such as MICROMEGAS [19] in conjunction with drone-based airborne muography.

References

[1] H. K. M. Tanaka *et al. High resolution imaging in the inhomogeneous crust with cosmic ray muon radiography: The density structure below the volcanic crater floor of Mt. Asama, Japan, Earth Planet. Sci. Lett.* **263** 104 (2007).

[2] H. K. M. Tanaka *et al. Detecting a mass change inside a volcano by cosmic-ray muon radiography (muography): First results from measurements at Asama volcano, Japan, Geophys. Res. Lett.,* **36** L17302 (2009).

[3] H. K. M. Tanaka *et al. Three dimensional CAT scan of a volcano with cosmic-ray muon radiography, Journal of Geophysical Research* **115** B12332 (2010).

[4] H. K. M. Tanaka *et al. Cosmic-ray muon imaging of magma in a conduit: degassing process of Satsuma-Iwojima Volcano, Japan, Geophys.Res. Lett.,* **36** L01304 (2009).

[5] H. K. M. Tanaka *et al. Radiographic visualization of magma dynamics in an erupting volcano Nature communications* **5**, 3381 (2014)

[6] H. K. M. Tanaka *et al. Imaging the conduit size of the dome with cosmic ray muons: The structure beneath Showa Shinzan Lava Dome, Japan, Geophys. Res. Lett.* **34** L22311 (2007).

[7] T. Kusagaya and H. K. M. Tanaka *Muographic imaging with a multi-layered telescope and its application to the study of the subsurface structure of a volcano. Proc Jpn Acad Ser B* **91** 501 (2015).

[8] H. K. M. Tanaka *Instant snapshot of the internal structure of Unzen lava dome, Japan with airborne muography. Sci. Rep.* **6** 39741 (2016).

[9] N. Lesparre *et al. Density Muon Radiography of La Soufrière of Guadeloupe Volcano: Comparison with Geological, Electrical Resistivity and Gravity data, Geophysical Journal International* **190** 1008 (2012).

[10] K. Jourde *et al. Muon dynamic radiography of density changes induced by hydrothermal activity at the La Soufrière of Guadeloupe volcano* **6**, 33406 (2016).

[11] C. Carloganu, *TOMUVOL muography project, MUOGRAPHERS 2016*, Tokyo, November 7, 2016. http://www.eri.u-tokyo.ac.jp/ht/MUOGRAPHERS16/General-Assembly/program.html

[12] V. Tioukov *et al. Muography with nuclear emulsions - Stromboli and other projects, Annals of Geophysics* **60**, S0111 (2017).

[13] D. Carbon *et al. An experiment of muon radiography at Mt Etna (Italy). Geophysical Journal International* **196** 633 (2014).

[14] O. Catalano, *ASTRI muography project, MUOGRAPHERS 2016*, Tokyo, November 7, 2016. http://www.eri.u-tokyo.ac.jp/ht/MUOGRAPHERS16/General-Assembly/program.html

[15] H. K. M. Tanaka *et al. Cosmic muon imaging of hidden seismic fault zones: Rainwater permeation into the mechanical fractured zones in Itoigawa–Shizuoka Tectonic Line, Japan, Earth Planet. Sc. Lett.* **306** 156 (2011).

[16] H. K. M. Tanaka, *Muographic mapping of the subsurface density structures in Miura, Boso and Izu peninsulas, Japan. Sci. Rep.* **5** 8305 (2015).

[17] L. W. Alvarez *et al. Search for hidden chambers in the pyramids, Science* **167**, 832 (1970).

[18] K. Morishima, *ScanPyramid muography project, MUOGRAPHERS 2016*, Tokyo, November 7, 2016. http://www.eri.u-tokyo.ac.jp/ht/MUOGRAPHERS16/General-Assembly/program.html

[19] S. Bouteille, *MICROMEGAS muography project, MUOGRAPHERS 2016*, Tokyo, November 7, 2016.

[20] G. Saracino, *Imaging underground cavities by cosmic-ray muons: observations at Mt Echia, Naples, Italy, MUOGRAPHERS 2016*, Tokyo, November 7, 2016. http://www.eri.u-tokyo.ac.jp/ht/MUOGRAPHERS16/General-Assembly/program.html

[21] H. K. M. Tanaka, *Development of stroboscopic muography, Geosci. Instrum. Method. Data Syst.* **2** 41 (2013).

[22] K. Morishima, *Muographic investigation of Fukushima nuclear power plant. Muography: Perspective Drawing in the 21st Century,* 87 (2015)

[23] E. P. George, *Cosmic rays measure overburden of tunnel, Commonwealth Engineer* **1 July** 455 (1955).

[24] T. Nakamura *et al., The OPERA film: New nuclear emulsion for large-scale, high-precision experiments, Nucl. Instrum. Meth. A* **556** 80 (2006).

[25] O.C. Allkofer *et al. Cosmic ray muon spectra at sea-level up to 10 TeV, Nuclear Physics B* **259**, 1 (1985)

[26] S. Haino *et al. Measurements of primary and atmospheric cosmic-ray spectra with the BESS-TeV spectrometer, Physics Letters B* **594** 35 (2004).

[27] H. Jokisch *et al. Cosmic-ray muon spectrum up to 1 TeV at 75° zenith angle, Phys. Rev. D* **19**, 1368 (1979).

[28] P. Achard *et al. Measurement of the atmospheric muon spectrum from 20 to 3000 GeV, Physics Letters B* **598** 15 (2004).

[29] S. Matsuno *et al. Cosmic-ray muon spectrum up to 20 TeV at 89° zenith angle Phys. Rev. D* **29**, 1 (1984).

[30] D.E. Groom *et al. Muon stopping-power and range tables: 10 MeV–100 TeV, Atomic Data and Nuclear Data Tables* **78** 183 (2001).

[31] Tanaka, H.K.M. *et al. Development of a portable assembly-type cosmic-ray muon module for measuring the density structure of a column of magma, Earth Planets Space* **62** 119 (2010).

[32] D. Varga, *REGARD muography project, MUOGRAPHERS 2016*, Tokyo, November 7, 2016.

[33] H. Taira and H. K. M. Tanaka, *A potential space- and power-effective muon sensor module for imaging a volcano, Earth Planets Space* **62** 179 (2010).

PoS(KMI2017)026